Endoplasmic Reticulum Stress Promotes LIPIN2-Dependent Hepatic Insulin Resistance

Dongryeol Ryu,[1] Woo-Young Seo,[1] Young-Sil Yoon,[1] Yo-Na Kim,[2] Su Sung Kim,[2] Hye-Jin Kim,[2] Tae-Sik Park,[2] Cheol Soo Choi,[1,2,3] and Seung-Hoi Koo[1]

OBJECTIVE—Diet-induced obesity (DIO) is linked to peripheral insulin resistance—a major predicament in type 2 diabetes. This study aims to identify the molecular mechanism by which DIO-triggered endoplasmic reticulum (ER) stress promotes hepatic insulin resistance in mouse models.

RESEARCH DESIGN AND METHODS—C57BL/6 mice and primary hepatocytes were used to evaluate the role of LIPIN2 in ER stress-induced hepatic insulin resistance. Tunicamycin, thapsigargin, and lipopolysaccharide were used to invoke acute ER stress conditions. To promote chronic ER stress, mice were fed with a high-fat diet for 8–12 weeks. To verify the role of LIPIN2 in hepatic insulin signaling, adenoviruses expressing wild-type or mutant LIPIN2, and shRNA for LIPIN2 were used in animal studies. Plasma glucose, insulin levels as well as hepatic free fatty acids, diacylglycerol (DAG), and triacylglycerol were assessed. Additionally, glucose tolerance, insulin tolerance, and pyruvate tolerance tests were performed to evaluate the metabolic phenotype of these mice.

RESULTS—LIPIN2 expression was enhanced in mouse livers by acute ER stress–inducers or by high-fat feeding. Transcriptional activation of LIPIN2 by ER stress is mediated by activating transcription factor 4, as demonstrated by LIPIN2 promoter assays, Western blot analyses, and chromatin immunoprecipitation assays. Knockdown of hepatic LIPIN2 in DIO mice reduced fasting hyperglycemia and improved hepatic insulin signaling. Conversely, overexpression of LIPIN2 impaired hepatic insulin signaling in a phosphatidic acid phosphatase activity–dependent manner.

CONCLUSIONS—These results demonstrate that ER stress–induced LIPIN2 would contribute to the perturbation of hepatic insulin signaling via a DAG-protein kinase C ε–dependent manner in DIO mice. *Diabetes* **60:1072–1081, 2011**

Excessive intake of diets rich in fat results in the increased incidence of obesity-associated peripheral insulin resistance. Accumulation of free fatty acids under this condition triggers the generation of second messengers such as diacylglycerol (DAG) and ceramide or their metabolites, which in turn

activates serine/threonine kinases that directly reduce insulin receptor/insulin receptor substrate–dependent signaling cascades in insulin-sensitive tissues, including the liver and muscle (1–3). Hyperglycemia is pronounced under the insulin resistance in part as a result of the uncontrolled hepatic glucose production, which would ultimately lead to the progression of type 2 diabetes (4).

Endoplasmic reticulum (ER) stress is elicited by conditions, such as inflammation and nutrient overloads that perturb normal ER homeostasis. Abnormal accumulation of unfolded proteins causes a collective signaling cascade termed unfolded protein response (UPR) in that setting, which leads to the release of GRP78 and the activation of three classes of signaling cascades to relieve such ER-associated stress (5): *1*) protein kinase RNA–like ER-associated kinase (PERK)-eukaryotic translation initiation factor 2α (eIF2α)-activating transcription factor 4 (ATF4) pathway; *2*) inositol-requiring protein 1α (IRE1α), X-box binding protein 1 (XBP1) pathway; and *3*) activating transcription factor 6 (ATF6) pathway.

Activation of PERK is critical in the attenuation of general translation under ER stress by phosphorylation/inactivation of eIF2α, and it also activates the translation of certain UPR gene clusters by activation of ATF4 (6). IRE1α uses its endoribonuclease activity to mediate a generation of splicing variants of XBP1, producing a potent basic leucine zipper (bZIP) transcriptional activator for enhancement of UPR genes (7). Finally, UPR also activates another bZIP transcription factor, ATF6, by promoting its proteolytic cleavage and liberation from the lumen of the ER. The resultant nuclear ATF6 can then enter into the nucleus and activate a subset of genes that are required for relieving ER stress conditions (8,9). Interestingly, although treatment of acute ER stress–inducers such as thapsigargin or tunicamycin could induce all of these signaling pathways in vitro, it was shown that only the PERK-dependent pathway is persistently activated under the obesity-induced chronic ER stress in rodents, suggesting the presence of a distinctive role for each pathway in response to differential stimuli in a physiological setting (10–13).

The LIPIN family of proteins constitutes the mammalian type 2 phosphatidic acid phosphatase (PAP) in mammals (14). LIPIN1, a founding member of this family, is linked to lipid metabolism and insulin signaling and is a gene product responsible for the pathophysiology of *fld* mice, presumably affecting the normal function of adipose tissues (15,16). Expression of LIPIN1 in the liver is less pronounced than in other tissues. However, multiple roles have been proposed for LIPIN1 in the regulation of hepatic lipid metabolism, suggesting that the hepatic function of this protein is critical for the mammalian lipid homeostasis. LIPIN1 possesses a coactivator activity for nuclear receptors such as peroxisome proliferator–activated

receptor α, and together with peroxisome proliferator–activated receptor coactivator-1α, could enhance fatty acid β-oxidations in the liver in the normal context (17). In addition, LIPIN1 might also be involved in the process of hepatic triacylglycerol (TAG) secretion in the normal physiological context, although the exact mechanism has not been elucidated to date (18,19). We have recently shown that LIPIN1 expression is significantly enhanced in the livers from mouse models of genetic obesity and diet-induced obesity (DIO), and its PAP function is critical in the progression of hepatic insulin resistance by promoting DAG-protein kinase C (PKC) ε–dependent inactivation of insulin receptor-mediated signaling cascades (20). These data suggest that abnormal regulation of LIPIN1 activity might be detrimental to the hepatic lipid homeostasis under pathophysiological conditions.

All three LIPIN proteins possess domains for PAP activity that are able to catalyze the conversion of phosphatidic acid to DAG, at least in vitro (21). Interestingly, LIPIN isoforms display differential tissue distributions. Whereas LIPIN1 is predominantly expressed in adipose tissues or muscle and less so in the liver and neuronal tissues, LIPIN2 is exclusively expressed in the liver and kidney. LIPIN3 is rather ubiquitously expressed, but its expression is almost absent in the liver, showing that this isoform may not function as an important PAP enzyme in the liver under physiological conditions (21,22). Although LIPIN2 is linked to the Majeed syndrome in humans, the exact physiological roles for LIPIN2 are not well studied in those clinical studies (23). Recently, LIPIN2 expression is also shown to be increased in the genetic mouse models of obesity (*ob/ob* and *db/db* mice), and is critical in the hepatic TAG production that is associated with its PAP activity (22), prompting us to investigate the exact molecular mechanism for the obesity-induced activation of LIPIN2 expression and its significance in the progression of insulin resistance in such conditions.

Here we report that LIPIN2 expression is induced by both acute and chronic ER stress conditions. ATF4, one of the major transcription factors that mediates ER stress-dependent signaling, is responsible for the transcriptional activation of LIPIN2 in the liver. Adenovirus-mediated knockdown of LIPIN2 in the liver greatly reduces hepatic DAG levels as well as hyperglycemia and insulin resistance in DIO mice. Conversely, overexpression of LIPIN2 promotes hepatic insulin resistance, which is associated with its PAP activity. These results demonstrate that chronic ER stress–induced LIPIN2 would contribute to the progression of hepatic insulin resistance in rodents.

RESEARCH DESIGN AND METHODS

Plasmids and recombinant adenoviruses. Promoter sequences for LIPIN2 were PCR-amplified from mouse genomic DNA and were inserted into the pGL4 basic vector (Promega). The coding sequence for mouse ATF4 was amplified from mouse hepatic cDNAs and inserted into pcDNA3-flag vectors to generate pcDNA3-flag-ATF4. The expression vector for dominant-negative ATF4 was generated as described (24). Adenoviruses for LIPIN2 and pcDNA3-flag-LIPIN2 were described previously (20). The LIPIN2 mutant (D712E, D714E) was selected based on the homology between LIPIN1 and LIPIN2 and was generated by site-directed mutagenesis as described (17,20). Adenoviruses expressing green fluorescent protein (GFP) only and the nonspecific RNA interference control (unspecific [US]) were described previously (25,26). Adenoviruses for ATF4 and short hairpin RNA for LIPIN2 (shLIPIN2) were generated as described previously (20,27).

Animal experiments. Four-week-old male C57BL/6 mice (for the DIO model) were purchased from Charles River Laboratories, and were fed a high-fat diet (60 kcal% fat diet; D12492 of Research Diets, Inc.) for 12 weeks in a specific pathogen-free facility at the Sungkyunkwan University School of Medicine

(12:12 h light-dark cycle). Recombinant adenovirus (0.5×10^9 plaque-forming units for overexpression, and 1×10^9 plaque-forming units for short hairpin RNA) was delivered by tail-vein injection. To measure fasting blood glucose levels, animals were fasted for 4 h with free access to water. For the glucose and pyruvate tolerance tests, mice were fasted for 4–16 h and then injected intraperitoneally with 2 g/kg body wt of glucose (on day 4 post-adenoviral injection) or pyruvate (on day 6 after adenoviral injection) (20). For the insulin tolerance test, mice were fasted for 4 h and then injected intraperitoneally with 1 unit/kg body wt of insulin on day 5 after adenoviral injection. Plasma glucose or insulin was measured on blood drawn from the tail vein at designated time points. To activate the insulin signaling pathway, either PBS (for control) or insulin (0.5 unit/kg body wt) was injected intraperitoneally for 10 min before the collection of the liver for further analyses on day 7 post-adenoviral injection. Seven-week-old male C57BL/6 mice (for the intraperitoneal injection of ER stress inducers) were purchased from Charles River Laboratories. ER stress was induced by intraperitoneal injection of tunicamycin (2.5 μg/g body wt for 2 h) or lipopolysaccharide (LPS) (3 μg/ g body wt for 8 h). All procedures were approved by the Sungkyunkwan University School of Medicine Institutional Animal Care And Use Committee (IACUC).

Quantitative PCR. Total RNA from either primary hepatocytes or mouse liver was extracted using RNeasy Mini Kit (Qiagen). cDNAs generated by Superscript II enzyme (Invitrogen) were analyzed by quantitative PCR using a SYBR green PCR kit and TP800, Thermal Cycler DICE Real Time System (TAKARA). All data were normalized to ribosomal L32 expression. Information for primers is described in Supplementary Table 1.

Western blot analyses. Whole cell extracts were prepared using radio-immunoprecipitation assay buffer containing protease inhibitor cocktails (Calbiochem). Western blot analyses on 50–100 μg of protein were performed as described (28). Information for antibodies is described in Supplementary Table 2.

Culture of primary hepatocytes. Primary hepatocytes were prepared from 6- to 8-week-old C57BL/6 mice as described previously (29). Cells were plated with medium 199 supplemented by 10% FBS, 10 units/mL penicillin, 10 μg/mL streptomycin, and 10 nmol/L dexamethasone. After attachment, cells were infected with various adenoviruses as indicated in figure legends. Subsequently, cells were maintained in the same media without FBS overnight and treated with 1.25 μg/mL tunicamycin, 0.5 μmol/L thapsigargin, 100 nmol/L phosphatidic acid, or 100 nmol/L insulin for designated time points in the figure legends.

Transfection assays. HepG2 cells were maintained with Ham's F12 medium supplemented with 10% FBS, 10 units/mL penicillin, and 10 μg/mL streptomycin. Each transfection was performed with 300 ng of luciferase construct, 50 ng of β-galactosidase plasmid, and 30–100 ng of expression vector for wild-type or dominant-negative ATF4 (24) using TransIT-LT1 transfection reagent (Mirus).

Chromatin immunoprecipitation assays. Nuclear isolation, cross-linking, and chromatin immunoprecipitation assays on primary mouse hepatocyte samples were performed as described previously (30). Precipitated DNA fragments were analyzed by PCR using primers against relevant mouse promoters.

Measurement of metabolites. For the measurement of metabolites, 4-h fasted mice were killed at day 7 post-adenoviral injection. Blood glucose for basal conditions and during glucose tolerance test was monitored from tail-vein blood using an automatic glucose monitor (One Touch, LifeScan). Hepatic lipids were extracted essentially as reported previously (31). Plasma and hepatic triglycerides and nonesterified fatty acids were measured by colorimetric assay kits (Wako). Insulin was measured by Mouse Insulin ELISA Kit (ALPCO). Hepatic DAGs were measured by liquid chromatography tandem mass spectometry with Atmosphere Pressure Chemical Ionization (APCI) source using homogenates from 30 mg of liver tissues as described (32).

Statistical analyses. Results are shown as mean ± SEM. The comparison of different groups was carried out using two-tailed unpaired Student *t* test, and differences at or under $P < 0.05$ were considered statistically significant and reported as in legends.

RESULTS

ER stress induces LIPIN2 expression in the liver. Recent reports indicated that unresolved ER stress could promote hepatic lipid synthesis by inducing key enzyme genes such as *SREBP-1c* and *DGAT2* (33), prompting us to investigate whether expression of LIPIN2, a liver-enriched mammalian PAP for DAG synthesis, is also affected. Tunicamycin or LPS induces expression of UPR genes such as *ATF4*, *CHOP*, *GRP78*, and the spliced form of *XBP1* in the mouse liver (Fig. 1*A* and *B*). Interestingly, we also observed enhanced expression of most lipogenic genes including *SREBP-1c*, *FAS*, and *LIPIN2*. Indeed, LIPIN2 protein levels are also enhanced under these
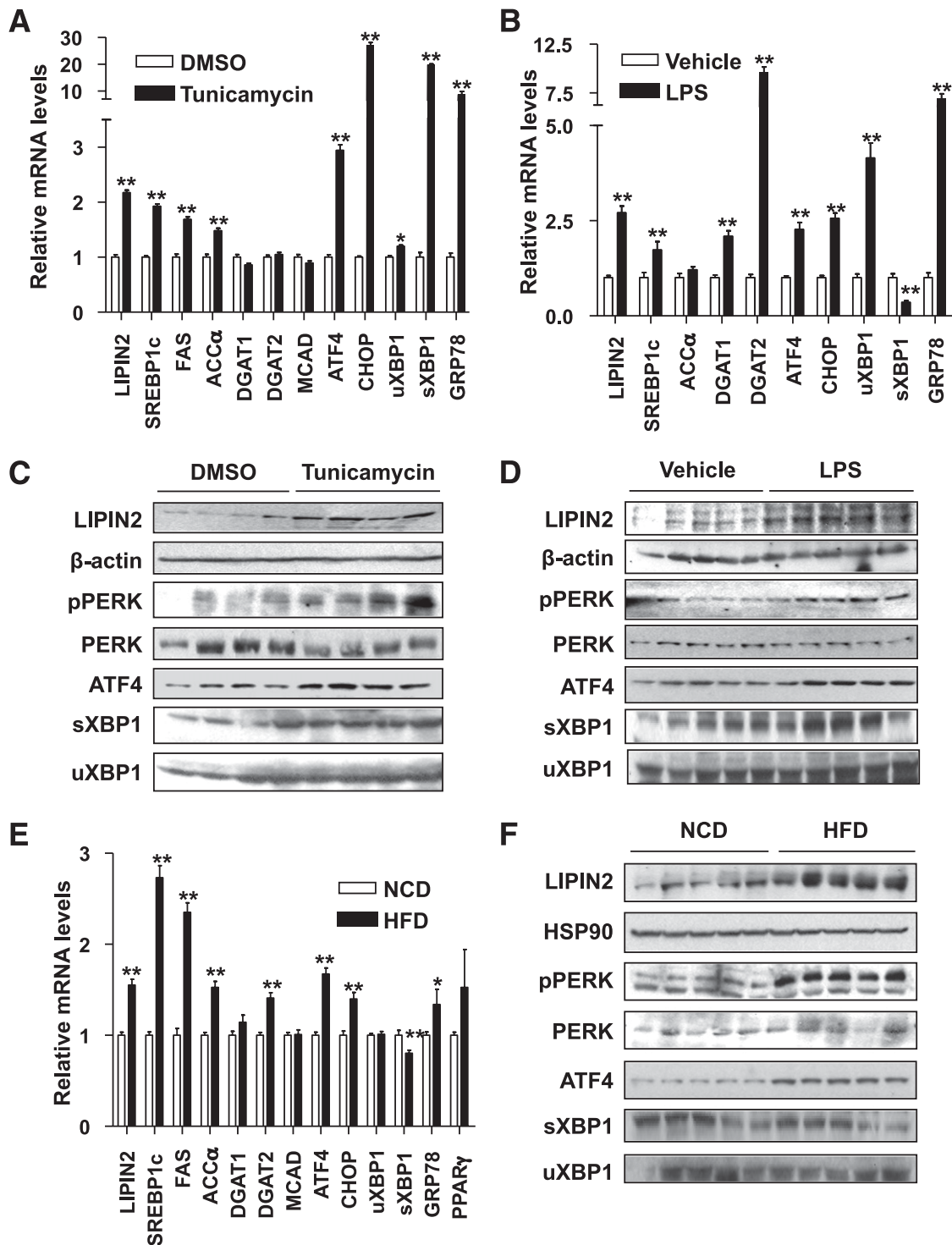
FIG. 1. ER stress induces LIPIN2 expression in vivo. *A*: Wild-type C57BL/6 mice were injected intraperitoneally with either DMSO or tunicamycin (2.5 μg per g body wt, *n* = 4 per group), and livers were collected 2 h post-injection. Quantitative PCR analysis was performed with hepatic RNAs. *B*: Saline (as a vehicle) or LPS (3 μg per g body wt, *n* = 5 per each group) was injected intraperitoneally, and livers were collected 8 h post-injection. Quantitative PCR analysis was performed with hepatic RNAs. *C*: Western blot analysis was performed with lysates from mouse livers as in *A*. Representative data from three independent experiments are shown. *D*: Western blot analysis was performed with lysates from mouse livers as in *B*. Representative data from three independent experiments are shown. *E* and *F*: Hepatic RNAs for quantitative PCR analysis (*E*) and lysates for Western blot assay (*F*) were prepared from mice on either normal chow diet or high-fat diet (60 kcal% fat for 12 weeks, D12492 [Research Diets] *n* = 5 per group). Representative data from three independent experiments are shown. Error bars indicate SEM. Statistical significance was assessed by two-tailed Student *t* test. *$P < 0.05$; **$P < 0.01$. sXBP1, spliced XBP1; uXBP1, unspliced XBP1.

conditions, suggesting that acute ER stress could promote DAG synthesis via activation of LIPIN2 (Fig. 1C and D and Supplementary Fig. 1). To verify the effect of ER stress on LIPIN2 expression in more physiological settings, we fed mice with a high-fat diet for 12 weeks to induce chronic ER stress conditions. Hepatic LIPIN2 expression is higher in high-fat diet–fed mice than in control mice (Fig. 1E and F and Supplementary Fig. 1). Interestingly, unlike the acute ER stress conditions, only a subset of UPR pathways (p-PERK, ATF4, CHOP) is activated under chronic conditions. These data suggest that both acute and chronic ER stress could induce LIPIN2 expression in the mouse liver.

ATF4 mediates ER stress–dependent activation of *LIPIN2* transcription. To directly test whether ER stress–mediated induction of *LIPIN2* expression is primarily via intrahepatic signaling pathways, we treated primary hepatocytes with tunicamycin or thapsigargin. Indeed, *LIPIN2* expression is enhanced by acute ER stress inducers (Fig. 2A and Supplementary Fig. 2). Next, we wanted to test whether ATF4 or CHOP, two transcription factors that are induced by both acute and chronic ER stress conditions, could activate *LIPIN2* expression. Because *CHOP* is a direct transcriptional target of ATF4, we prepared expression plasmids for ATF4 and CHOP, and transfected each construct in the cultured cells. Overexpression of CHOP does not significantly induce *LIPIN2* expression. On the other hand, overexpression of ATF4 enhances protein levels of LIPIN2, suggesting that ATF4, but not CHOP, is responsible for promoting expression of *LIPIN2* (Supplementary Fig. 3). Infection of adenovirus for ATF4 also mimics the effect of ER stress–dependent induction of *LIPIN2* mRNA, supporting the notion that ATF4 could function as a transcriptional activator that mediates ER stress–dependent induction of *LIPIN2* expression in hepatocytes (Fig. 2B). To further determine whether ATF4 could regulate *LIPIN2* expression at the transcription level, we performed LIPIN2 reporter assays. We observed about threefold induction of LIPIN2 promoter activity by thapsigargin treatment (Fig. 2C). Further deletion analysis reveals that ATF4 can activate promoter activity of mouse LIPIN2 (Fig. 2D), which is inhibited by cotransfection of ATF4-DN (Supplementary Fig. 4). Finally, occupancy of ATF4 over its binding site on the LIPIN2 promoter was confirmed by chromatin immunoprecipitation assay, and ATF4 binding is enhanced significantly both by thapsigargin and tunicamycin treatment (Fig. 2E and F). These data support the notion that ER stress–dependent induction of *LIPIN2* is mediated mainly by ATF4 at the transcription level.

Depletion of LIPIN2 reduces glucose intolerance and improves insulin sensitivity. Next, we wanted to address whether elevated expression of LIPIN2 plays a role in ER stress–dependent signalings in mice. To this end, we generated adenovirus-expressing shLIPIN2 (Ad shLIPIN2) and injected it into mice. Knockdown of LIPIN2 in normal chow-fed mice slightly reduces blood glucose levels or hepatic triglyceride levels, although the values do not reach statistical significance (Supplementary Fig. 5). We thus attempted to test the Ad shLIPIN2 in high-fat diet–fed mice, in which hepatic LIPIN2 expression is elevated. Indeed, knockdown of hepatic LIPIN2 in high-fat diet–fed mice reduces hepatic triglyceride and DAG levels without affecting plasma free fatty acids or triglyceride levels (Fig. 3A–F). Furthermore, plasma glucose and insulin levels are reduced upon LIPIN2 knockdown, suggesting that LIPIN2 might be involved in the perturbation of insulin signaling in response to high fat–induced chronic ER stress conditions

in the liver (Fig. 3G and H). This notion was further confirmed by glucose and insulin tolerance tests, as these tests revealed that LIPIN2 knockdown improves glucose intolerance or insulin resistance in high-fat diet–fed mice (Fig. 4A–C and Supplementary Fig. 6). Of note, plasma insulin levels between control and LIPIN2-knockdown animals are not significantly different during the glucose tolerance test, showing that improved glucose tolerance upon LIPIN2 knockdown might stem from the enhanced ability to clear excessive plasma glucose without affecting insulin secretion (Fig. 4B). Depletion of LIPIN2 also reduces hepatic glucose production in response to the injection of gluconeogenic precursors and expression levels for gluconeogenic enzymes, showing a sign of restoration in glucose homeostasis in this setting (Fig. 4D and E and Supplementary Fig. 7).

Improvement of insulin signaling by LIPIN2 knockdown was verified by Western blot analysis, which showed the increased tyrosine phosphorylation of insulin receptor or insulin receptor substrate 1, serine phosphorylation of AKT and GSK3β, and diminished serine phosphorylation of PKCε (Fig. 4E and Supplementary Fig. 7). On the other hand, tyrosine phosphorylation of insulin receptor substrate 2 or p85 levels are not significantly affected by LIPIN2 knockdown, perhaps reflecting the presence of a residual PAP activity by other LIPIN isoforms. In line with this notion, knockdown of LIPIN2 does not affect the expression of LIPIN1, which may explain the incomplete activation of insulin signaling with the acute depletion of hepatic LIPIN2 (Supplementary Fig. 8). Similar effect on insulin signaling is also obtained by LIPIN2 knockdown in primary hepatocytes in the presence of phosphatidic acid, further corroborating the notion that hepatic LIPIN2 knockdown improves insulin sensitivity in insulin resistant conditions (Supplementary Figs. 9 and 10).

PAP activity of LIPIN2 is critical in the promotion of hepatic insulin resistance. Next, we attempted to verify the importance of PAP function of LIPIN2 in perturbing hepatic lipid metabolism and insulin signaling under the ER stress conditions. To this end, we generated adenovirus for wild-type or PAP-mutant LIPIN2 and inject each virus into the mice. Overexpression of LIPIN2 does not invoke significant changes in blood glucose levels or hepatic triglyceride levels in normal chow-fed mice compared with PAP mutant LIPIN2 (Supplementary Fig. 11), suggesting that the presence of a fatty acid–derived precursor such as phosphatidic acid is critical for the full PAP activity of LIPIN2. Indeed, hepatic expression of wild-type LIPIN2, but not mutant LIPIN2, results in higher DAG and triglyceride levels in the mouse liver without affecting the plasma fatty acids or triglyceride levels in a PAP function–dependent manner in high-fat diet–fed mice (Fig. 5A–F).

Expression of LIPIN2 also promotes hyperglycemia and hyperinsulinemia and perturbs glucose tolerance and insulin sensitivity (Figs. 5G and H and 6A–C), presumably as a result of the impaired insulin signaling, as evidenced by reduced tyrosine phosphorylation of insulin receptor, insulin receptor substrate 1, insulin receptor substrate 2, p85 levels, serine phosphorylation of AKT, enhanced serine phosphorylation of PKCε and expression of gluconeogenic enzymes in LIPIN2 mice compared with mice infected with mutant LIPIN2 or GFP control adenovirus (Fig. 6D and Supplementary Fig. 12). Unlike the case for LIPIN2 knockdown, we observed that tyrosine phosphorylation of both insulin receptor substrate 1 and insulin receptor substrate 2 are similarly affected by LIPIN2 overexpression,
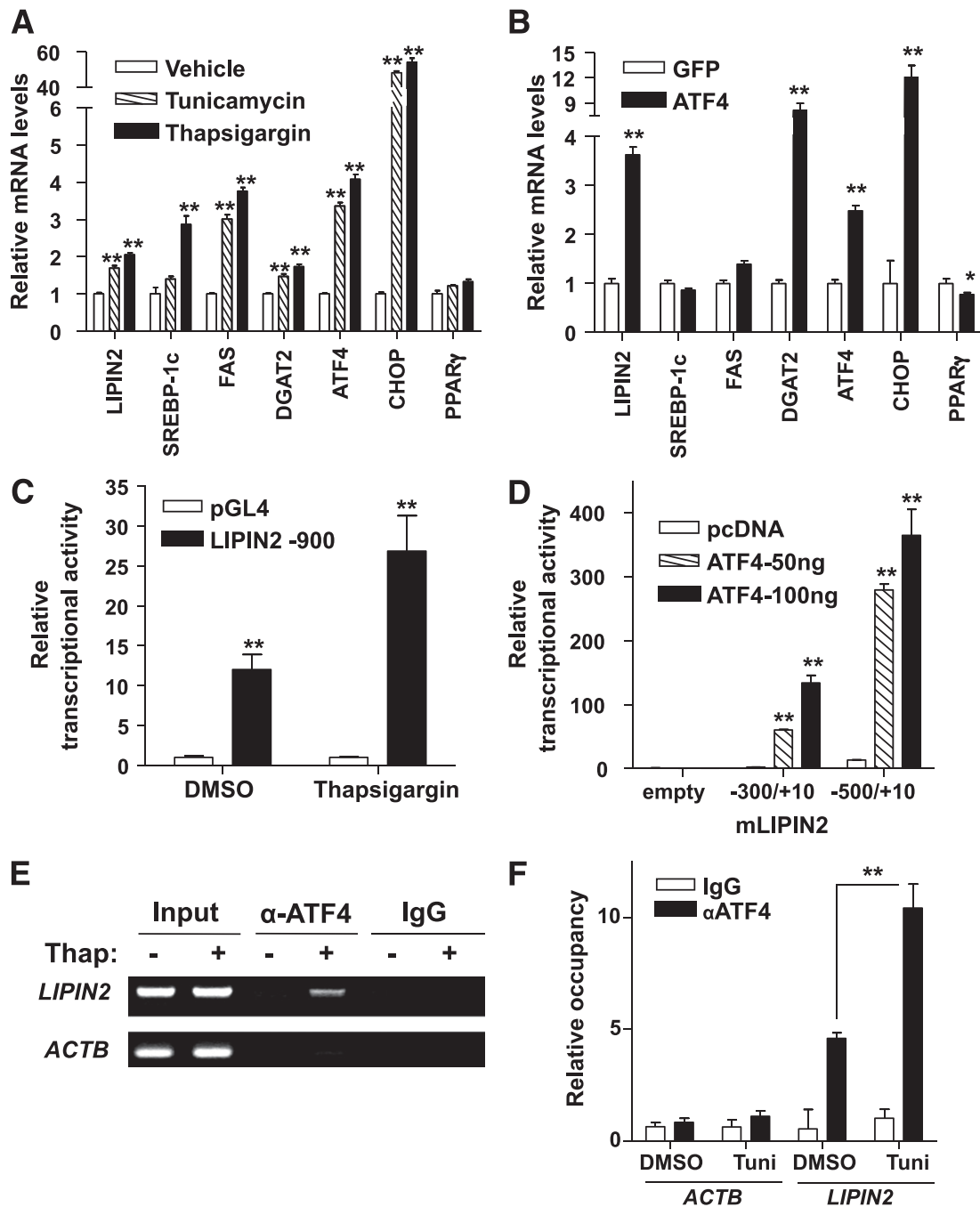
FIG. 2. ATF4 mediates ER stress–induced expression of LIPIN2. *A*: Quantitative PCR analysis was performed with RNAs from mouse primary hepatocytes. Cells were treated with DMSO, tunicamycin (1.25 μg/mL), or thapsigargin (0.5 μmol/L) for 24 h before being harvested. Representative data from four independent experiments are shown (*n* = 3 samples per group). *B*: Quantitative PCR analysis was performed with RNAs from primary hepatocytes infected with either GFP control or ATF4 adenovirus (multiplicity of infection = 50) for 48 h. Representative data from three independent experiments are shown (*n* = 3 samples per group). *C* and *D*: Luciferase assays of HepG2 cells transiently transfected with LIPIN2 reporter constructs. Cells were either treated with 0.5 μmol/L thapsigargin for 24 h (*C*), or cotransfected with 50 or 100 ng of ATF4 expression plasmid for 48 h (*D*). Representative data from three independent experiments are shown (*n* = 3 samples per group). *E*: Chromatin immuno-precipitation assay represents the occupancy of ATF4 on the LIPIN2 promoter in mouse primary hepatocytes. Thapsigargin (0.5 μmol/L) was treated for 2 h. *F*: Quantitative PCR analysis for chromatin immunoprecipitation assay using liver lysates of wild-type mice. C57BL/6 mice were injected intraperitoneally with either DMSO or tunicamycin (2.5 μg per g body wt, *n* = 3 per group), and livers were collected 2 h post-injection. Error bars indicate SEM. Statistical significance was assessed by two-tailed Student *t* test. *$P < 0.05$; **$P < 0.01$. Tuni, tunicamycin.

reflecting the severity of insulin resistance caused by the presence of supra-physiological levels of LIPIN2 in the liver. Again, plasma insulin levels during the GTT are not significantly different between mice with GFP, wild type or mutant LIPIN2 (Fig. 6*B*). Similarly, insulin-dependent increase in serine phosphorylation of AKT is reduced upon overexpression of enzymatically active LIPIN2 in primary hepatocytes in response to phosphatidic acid treatment (Supplementary Fig. 13). Collectively, these data suggest that PAP function of LIPIN2 is critical in enhancing DAG-PKCε–dependent signals to inhibit hepatic insulin signaling pathway in mammals with DIO.
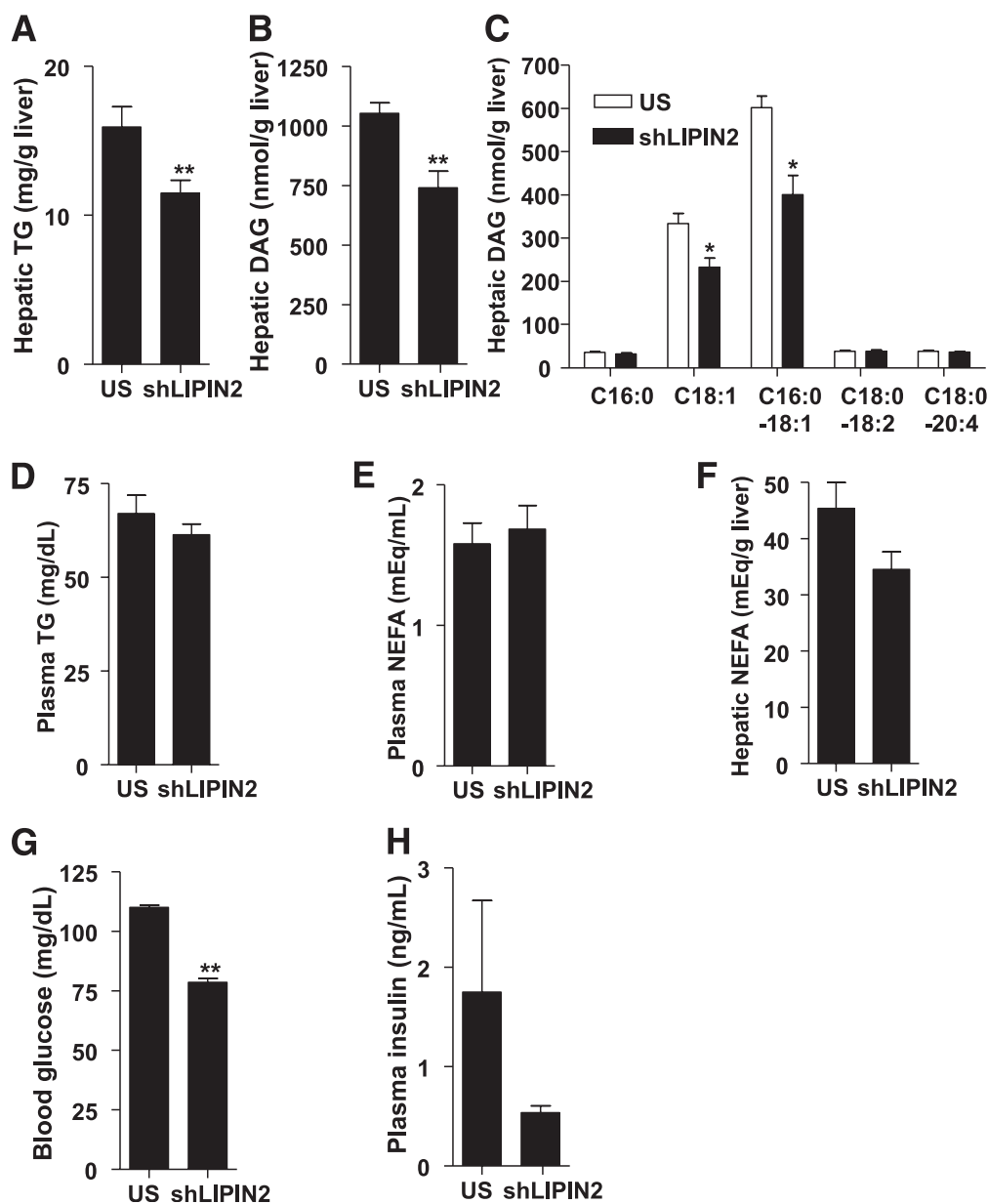
FIG. 3. LIPIN2 deficiency reduces hyperglycemia and improves fatty liver in DIO mice. *A*: Four-hour fasting hepatic TAG levels (n = 10 for US and n = 9 for shLIPIN2) from 12-week high-fat diet–fed mice that were injected with either Ad US (control) or Ad shLIPIN2 adenovirus. *B* and *C*: Four-hour fasting hepatic DAG levels from mice as in *A* (n = 9 for US and n = 8 for shLIPIN2) (for total hepatic DAG levels [*B*] and for individual classes of hepatic DAG [*C*]). *D–F*: Plasma TAG (*D*), plasma nonesterified fatty acid (*E*), and hepatic nonesterified fatty acid (*F*) levels from mice as in *A* (n = 10 for US and n = 9 for shLIPIN2). *G*: Four-hour fasting plasma glucose levels from 12-week high-fat diet–fed mice injected with either Ad US (control) or Ad shLIPIN2 adenovirus (n = 9 per each group). *H*: Four-hour fasting plasma insulin levels from 12-week high-fat diet–fed mice injected with either Ad US (control) or Ad shLIPIN2 adenovirus (n = 3 for US, n = 4 for shLIPIN2). For the measurement of metabolites, 4-h fasted mice were killed at day 7 after adenoviral injection. Error bars indicate SEM. Statistical significance was assessed by two-tailed Student t test. *P < 0.05; **P < 0.01. TG, triglyceride.

DISCUSSION

ER stress has been linked to insulin resistance and metabolic syndrome (34,35). Under conditions of physiological ER stress such as over-nutrition or bacterial/viral infection, UPR signaling in the liver is normally activated to restore ER homeostasis. Prolonged ER stress might cause irreversible defects in UPR signaling, and unresolved ER stress would perturb lipid homeostasis to produce cellular second messengers such as DAG or ceramides, and promote insulin resistance in the liver. ER stress–dependent activation of transcription factors, such as ATF6, XBP1

and ATF4, have been implicated in this phenomenon both in cultured cells and in vivo animal models.

Recent findings suggested that not all ER stress–linked transcription factors are equally activated both in acute and chronic ER stress conditions. Indeed, nuclear ATF6 and XBP1 levels in the liver are both diminished in diet-induced or genetic mouse models of obesity, indicating that these factors may not be actively involved in the progression of insulin resistance under chronic ER stress conditions (10–12). Moreover, nuclear XBP1 is critical in activating normal PI3 kinase–dependent signaling cascades,
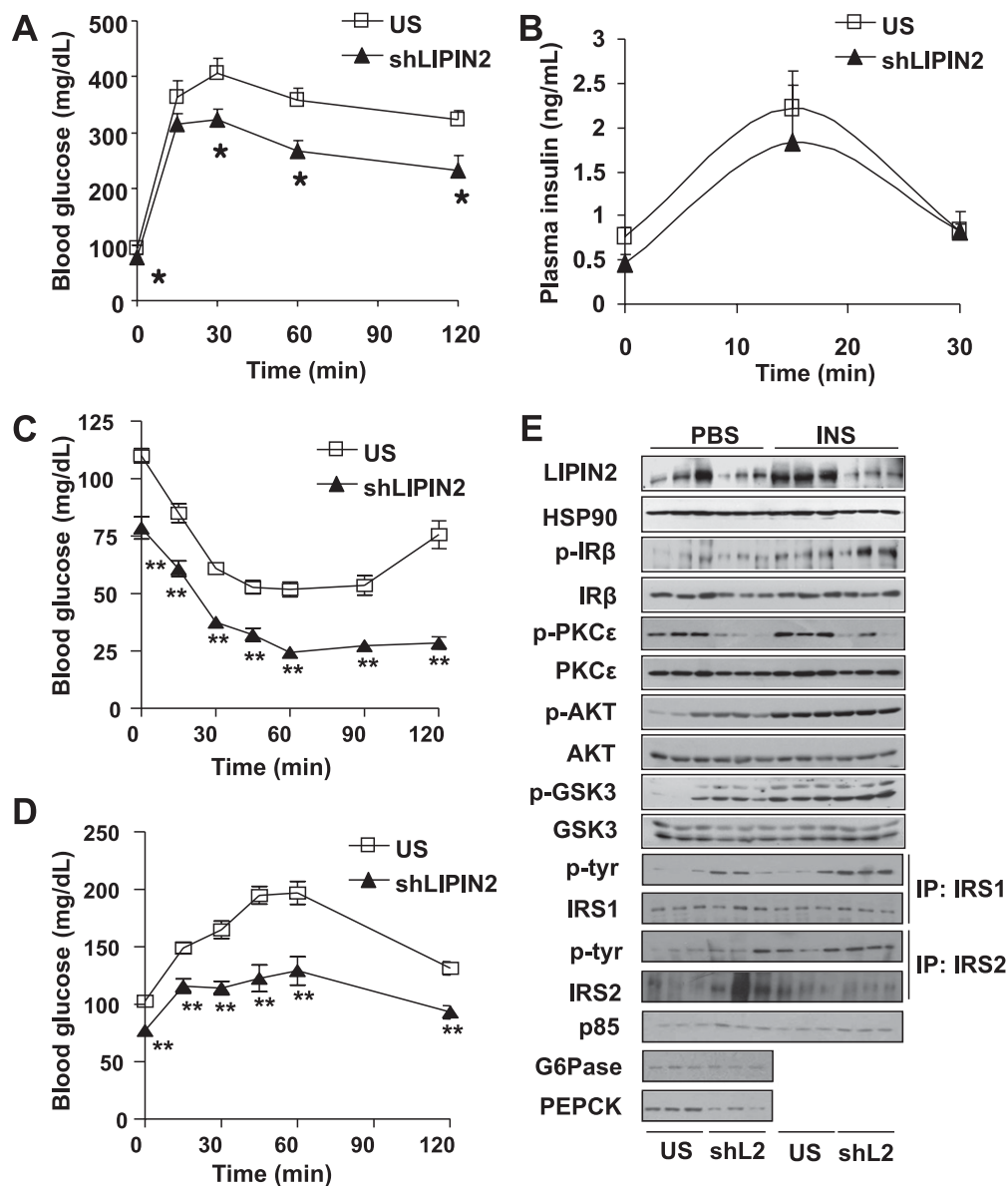
FIG. 4. LIPIN2 deficiency in DIO mice improves glucose intolerance and insulin sensitivity. *A–D*: Glucose tolerance test (*A*) (2 g glucose per kg body wt, *n* = 10 for US and *n* = 7 for shLIPIN2, using 4-h fasted mice at day 4 after adenoviral injection), plasma insulin levels during the glucose tolerance (*B*), insulin tolerance (*C*) (1 unit insulin per kg body wt, *n* = 9 per each group, at day 5 after adenoviral injection), and pyruvate challenge tests (*D*) (1 g glucose per kg body wt, *n* = 9 per each group, at day 4 after adenoviral injection) from mice as in Fig. 3. *E*: Western blot assays using lysates from either Ad US– or Ad shLIPIN2–infected mouse livers as in Fig. 3. PBS (for control) or insulin (0.5 unit/kg body wt) was injected intraperitoneally for 10 min before the collection of liver for Western blot assays on day 7 after adenoviral injection. Representative data from two independent experiments (*n* = 6 for each condition) are shown. Error bars indicate SEM. Statistical significance was assessed by two-tailed Student *t* test. *$P < 0.05$; **$P < 0.01$.

and reduction of this factor in the nucleus might be a critical initiator for hepatic insulin resistance in diet-induced or genetic mouse models of obesity.

On the other hand, hepatic ATF4 expression is shown to be increased upon high-fat diet (Fig. 1*E* and *F*). Furthermore, ATF4 knock-out mice were resistant to DIO associated with increased lipid oxidation and reduced glucose intolerance (36,37). Thus, it is plausible to speculate that chronic ER stress–induced activation of ATF4 or its downstream transcription factor CHOP would be in part responsible for the promotion of hepatic insulin resistance under the chronic ER stress condition such as DIO. It is noteworthy to mention that the involvement of other ER stress–induced pathways under different pathological stimuli or in nonhepatic tissues

should also be considered in the progression of insulin resistance to understand more completely the pathophysiological consequences of chronic ER stress.

In this study, we demonstrated that hepatic LIPIN2 is critical in ER stress–dependent regulation of lipid homeostasis and insulin resistance in mouse models of DIO (Fig. 6*E* for a proposed model). Both acute and chronic ER stress conditions promote increased *LIPIN2* transcription via ATF4-dependent machineries. Although knockdown of LIPIN2 in the liver ameliorates hepatic insulin resistance and reduces hyperglycemic phenotypes in DIO mice, overexpression of LIPIN2 with intact PAP activity greatly promotes insulin resistance by inducing DAG production and activity of PKCε in the mouse liver. Activation of PKCε
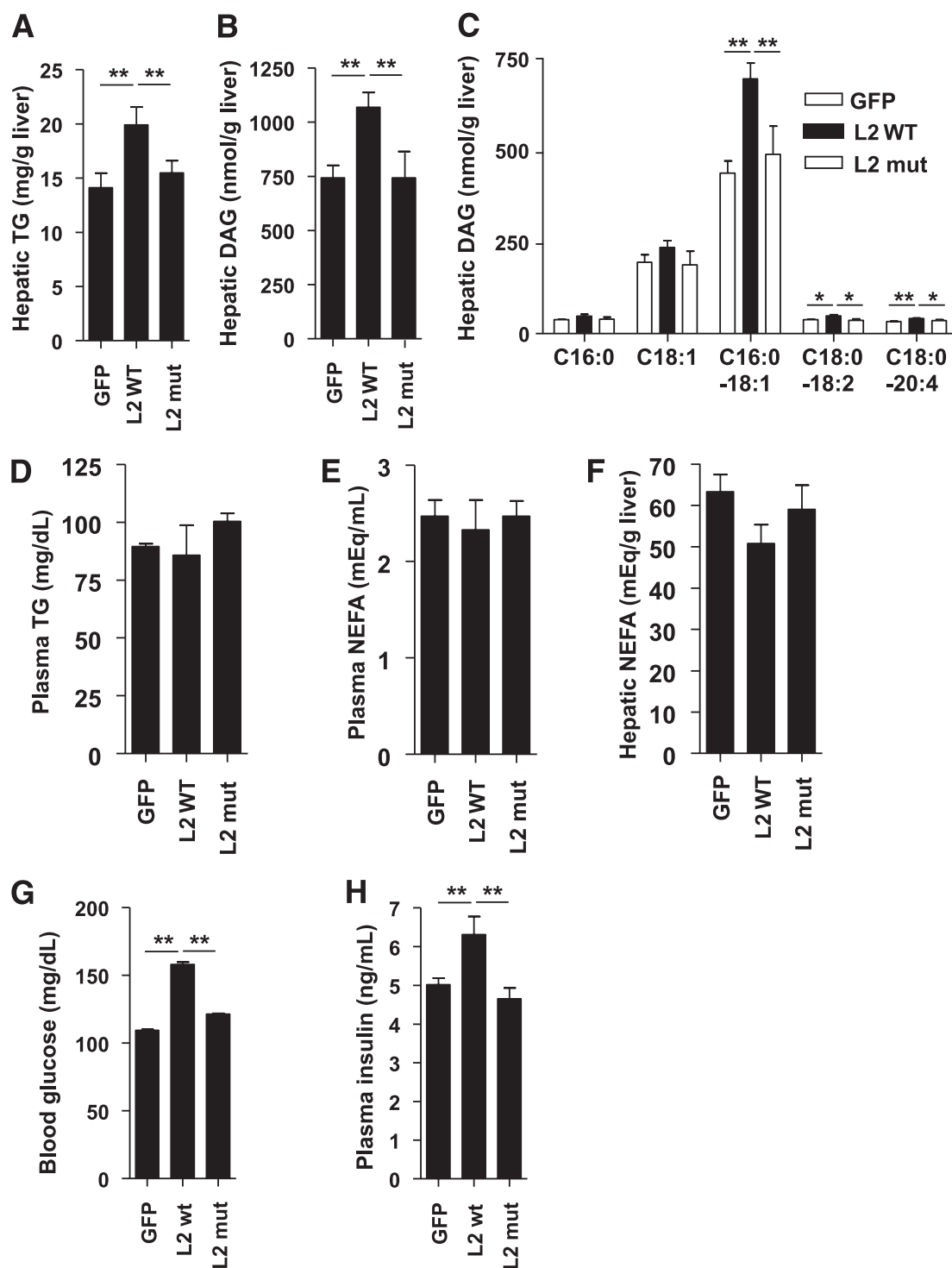
FIG. 5. Overexpression of LIPIN2 deteriorates glucose and lipid homeostasis in DIO mice. *A*: Four-hour fasting hepatic TAG (*n* = 8 for GFP and mutant LIPIN2 [L2 mut], and *n* = 9 for wild-type LIPIN2 [L2 wt]) from 12-week high-fat diet–fed mice injected with Ad GFP, Ad wild-type LIPIN2, or Ad mutant LIPIN2. *B* and *C*: Four-hour fasting hepatic DAG levels from 12-week high-fat diet–fed mice infected with Ad GFP, Ad wild-type LIPIN2, or Ad mutant LIPIN2 adenovirus (*n* = 7 for GFP and mutant LIPIN2 and *n* = 8 for wild-type LIPIN2) (for total hepatic DAG levels [*B*] and for individual classes of hepatic DAG [*C*]). *D–F*: Plasma TAG (*D*), plasma nonesterified fatty acid (*E*), and hepatic nonesterified fatty acid (*F*) levels from mice as in *A* (*n* = 8 for GFP and mutant LIPIN2, and *n* = 9 for wild-type LIPIN2). *G* and *H*: Four-hour fasting blood glucose (*G*) (*n* = 8 for GFP and mutant LIPIN2, and *n* = 9 for wild-type LIPIN2) or 4-h fasting plasma insulin (*H*) (*n* = 4 for each group) was measured from 12-week high-fat diet–fed mice injected with Ad GFP, Ad wild-type LIPIN2, or Ad mutant LIPIN2. For the measurement of metabolites, 4-h fasted mice were killed at day 7 after adenoviral injection. Error bars indicate SEM. Statistical significance was assessed by two-tailed Student *t* test. *$P < 0.05$; **$P < 0.01$. TG, triglyceride.
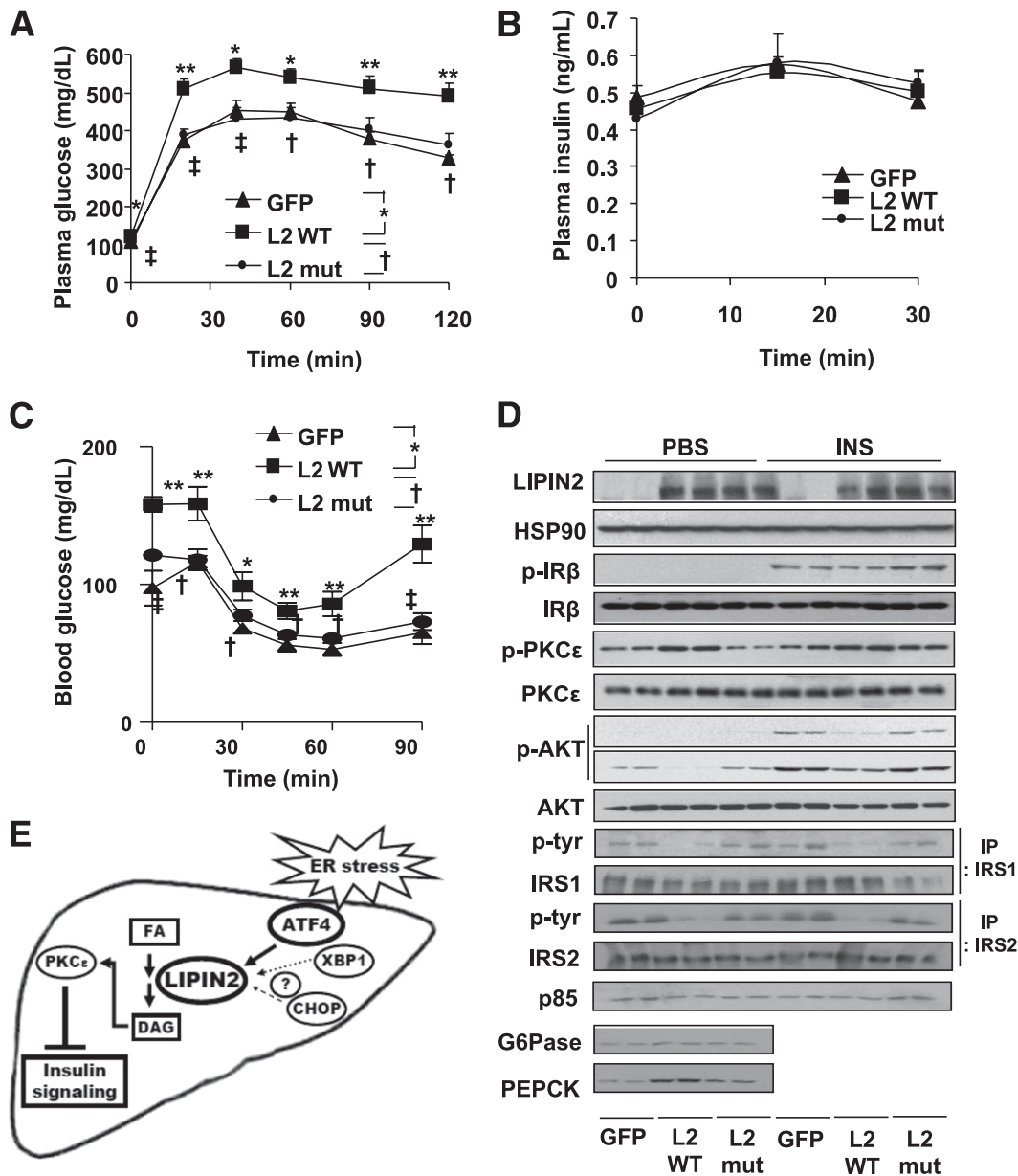
FIG. 6. Overexpression of LIPIN2 perturbs hepatic insulin signaling in DIO mice. *A–C*: Glucose tolerance test (*A*) (2 g glucose per kg body wt, *n* = 6 for GFP and *n* = 7 for wild-type and mutant LIPIN2, using 16-h fasted mice at day 4 after adenoviral injection), plasma insulin levels during glucose tolerance test (*B*), and insulin tolerance test (*C*) (1 unit insulin per kg body wt, *n* = 8 for GFP and mutant LIPIN2 mutant, and *n* = 9 for wild-type LIPIN2, at day 5 after adenoviral injection) from mice as in Fig. 5. *D*: Western blot assay using lysates from Ad GFP, Ad wild-type LIPIN2 (L2 wt), or Ad mutant LIPIN2 (L2 mut) infected mouse livers as in Fig. 5. PBS (for control) or insulin (0.5 unit/kg body wt) was injected intraperitoneally for 10 min before the collection of liver for Western blot assays on day 7 after adenoviral injection. Representative data from three independent experiments (*n* = 6 for each condition) are shown. *E*: A proposed model for ER stress–induced activation of LIPIN2 in promoting DAG production and the perturbation of hepatic insulin signaling. Error bars indicate SEM. Statistical significance was assessed by two-tailed Student *t* test. *$P < 0.05$; **$P < 0.01$; †$P < 0.05$; ‡$P < 0.01$.

then leads to the inactivation of insulin receptor–dependent signaling cascades, which is in line with previous reports showing that free fatty acid–dependent activation of PKCε inhibits insulin receptor activity by a direct protein-protein interaction (2,38). Interestingly, neither knockdown nor overexpression of LIPIN2 greatly affects hepatic glucose or lipid metabolism in normal chow-fed mice, suggesting that the presence of adequate substrate (e.g., increased hepatic fatty acid concentration due to over-nutrition rich in fat) is prerequisite for the generation of excessive DAG, which plays a role as a second messenger to perturb insulin signaling. These data would illustrate the critical role of LIPIN2 in mediating ER stress–dependent lipid accumulation and the promotion of hepatic insulin resistance. Given the predominant expression of LIPIN2 in the liver, it is plausible to suggest that targeted disruption or selective inactivation of this isoform is helpful to restore the normal insulin signaling and glycemia under the chronic ER stress condition.

REFERENCES

1. Jaeschke A, Davis RJ. Metabolic stress signaling mediated by mixed-lineage kinases. Mol Cell 2007;27:498–508
2. Samuel VT, Liu ZX, Wang A, et al. Inhibition of protein kinase Cepsilon prevents hepatic insulin resistance in nonalcoholic fatty liver disease. J Clin Invest 2007;117:739–745
3. Um SH, D'Alessio D, Thomas G. Nutrient overload, insulin resistance, and ribosomal protein S6 kinase 1, S6K1. Cell Metab 2006;3:393–402
4. Saltiel AR, Kahn CR. Insulin signalling and the regulation of glucose and lipid metabolism. Nature 2001;414:799–806
5. Schröder M, Kaufman RJ. The mammalian unfolded protein response. Annu Rev Biochem 2005;74:739–789
6. Harding HP, Zhang Y, Zeng H, et al. An integrated stress response regulates amino acid metabolism and resistance to oxidative stress. Mol Cell 2003; 11:619–633
7. Yoshida H, Matsui T, Yamamoto A, Okada T, Mori K. XBP1 mRNA is induced by ATF6 and spliced by IRE1 in response to ER stress to produce a highly active transcription factor. Cell 2001;107:881–891
8. Chen X, Shen J, Prywes R. The luminal domain of ATF6 senses endoplasmic reticulum (ER) stress and causes translocation of ATF6 from the ER to the Golgi. J Biol Chem 2002;277:13045–13052
9. Shen J, Chen X, Hendershot L, Prywes R. ER stress regulation of ATF6 localization by dissociation of BiP/GRP78 binding and unmasking of Golgi localization signals. Dev Cell 2002;3:99–111
10. Winnay JN, Boucher J, Mori MA, Ueki K, Kahn CR. A regulatory subunit of phosphoinositide 3-kinase increases the nuclear accumulation of X-box-binding protein-1 to modulate the unfolded protein response. Nat Med 2010;16:438–445
11. Park SW, Zhou Y, Lee J, et al. The regulatory subunits of PI3K, p85alpha and p85beta, interact with XBP-1 and increase its nuclear translocation. Nat Med 2010;16:429–437
12. Wang Y, Vera L, Fischer WH, Montminy M. The CREB coactivator CRTC2 links hepatic ER stress and fasting gluconeogenesis. Nature 2009;460:534–537
13. Ozcan U, Cao Q, Yilmaz E, et al. Endoplasmic reticulum stress links obesity, insulin action, and type 2 diabetes. Science 2004;306:457–461
14. Reue K, Dwyer JR. Lipin proteins and metabolic homeostasis. J Lipid Res 2009;50 (Suppl.):S109–S114
15. Péterfy M, Phan J, Xu P, Reue K. Lipodystrophy in the fld mouse results from mutation of a new gene encoding a nuclear protein, lipin. Nat Genet 2001;27:121–124
16. Phan J, Reue K. Lipin, a lipodystrophy and obesity gene. Cell Metab 2005;1: 73–83
17. Finck BN, Gropler MC, Chen Z, et al. Lipin 1 is an inducible amplifier of the hepatic PGC-1alpha/PPARalpha regulatory pathway. Cell Metab 2006;4: 199–210
18. Chen Z, Gropler MC, Norris J, Lawrence JC Jr, Harris TE, Finck BN. Alterations in hepatic metabolism in fld mice reveal a role for lipin 1 in regulating VLDL-triacylglyceride secretion. Arterioscler Thromb Vasc Biol 2008;28:1738–1744
19. Bou Khalil M, Sundaram M, Zhang HY, et al. The level and compartmentalization of phosphatidate phosphatase-1 (lipin-1) control the assembly and secretion of hepatic VLDL. J Lipid Res 2009;50:47–58
20. Ryu D, Oh KJ, Jo HY, et al. TORC2 regulates hepatic insulin signaling via a mammalian phosphatidic acid phosphatase, LIPIN1. Cell Metab 2009;9: 240–251
21. Donkor J, Sariahmetoglu M, Dewald J, Brindley DN, Reue K. Three mammalian lipins act as phosphatidate phosphatases with distinct tissue expression patterns. J Biol Chem 2007;282:3450–3457
22. Gropler MC, Harris TE, Hall AM, et al. Lipin 2 is a liver-enriched phosphatidate phosphohydrolase enzyme that is dynamically regulated by fasting and obesity in mice. J Biol Chem 2009;284:6763–6772
23. Reue K. The lipin family: mutations and metabolism. Curr Opin Lipidol 2009;20:165–170
24. He CH, Gong P, Hu B, et al. Identification of activating transcription factor 4 (ATF4) as an Nrf2-interacting protein. Implication for heme oxygenase-1 gene regulation. J Biol Chem 2001;276:20858–20865
25. Herzig S, Hedrick S, Morantte I, Koo SH, Galimi F, Montminy M. CREB controls hepatic lipid metabolism through nuclear hormone receptor PPAR-gamma. Nature 2003;426:190–193
26. Herzig S, Long F, Jhala US, et al. CREB regulates hepatic gluconeogenesis through the coactivator PGC-1. Nature 2001;413:179–183
27. He TC, Zhou S, da Costa LT, Yu J, Kinzler KW, Vogelstein B. A simplified system for generating recombinant adenoviruses. Proc Natl Acad Sci USA 1998;95:2509–2514
28. Michael LF, Asahara H, Shulman AI, Kraus WL, Montminy M. The phosphorylation status of a cyclic AMP-responsive activator is modulated via a chromatin-dependent mechanism. Mol Cell Biol 2000;20:1596–1603
29. Renton KW, Deloria LB, Mannering GJ. Effects of polyriboinosinic acid polyribocytidylic acid and a mouse interferon preparation on cytochrome P-450-dependent monooxygenase systems in cultures of primary mouse hepatocytes. Mol Pharmacol 1978;14:672–681
30. Shang Y, Hu X, DiRenzo J, Lazar MA, Brown M. Cofactor dynamics and sufficiency in estrogen receptor-regulated transcription. Cell 2000;103: 843–852
31. Folch J, Lees M, Sloane Stanley GH. A simple method for the isolation and purification of total lipides from animal tissues. J Biol Chem 1957;226: 497–509
32. Bligh EG, Dyer WJ. A rapid method of total lipid extraction and purification. Can J Biochem Physiol 1959;37:911–917
33. Glimcher LH, Lee AH. From sugar to fat: How the transcription factor XBP1 regulates hepatic lipogenesis. Ann N Y Acad Sci 2009;1173(Suppl 1): E2–E9
34. Hotamisligil GS. Endoplasmic reticulum stress and atherosclerosis. Nat Med 2010;16:396–399
35. Hotamisligil GS. Endoplasmic reticulum stress and the inflammatory basis of metabolic disease. Cell 2010;140:900–917
36. Seo J, Fortuno ES 3rd, Suh JM, et al. Atf4 regulates obesity, glucose homeostasis, and energy expenditure. Diabetes 2009;58:2565–2573
37. Wang C, Huang Z, Du Y, Cheng Y, Chen S, Guo F. ATF4 regulates lipid metabolism and thermogenesis. Cell Res 2010;20:174–184
38. Pillay TS, Xiao S, Keranen L, Olefsky JM. Regulation of the insulin receptor by protein kinase C isoenzymes: preferential interaction with beta isoenzymes and interaction with the catalytic domain of betaII. Cell Signal 2004;16:97–104